

罗文军,季少聪,刘曦翔,等.四川盆地高石梯—磨溪地区震旦系灯影组白云岩溶蚀差异实验研究[J].中国岩溶,2023,42(6):1312-1321.

DOI: [10.11932/karst20230612](https://doi.org/10.11932/karst20230612)

四川盆地高石梯—磨溪地区震旦系灯影组 白云岩溶蚀差异实验研究

罗文军¹,季少聪^{2,3},刘曦翔¹,淡永^{2,3},梁彬^{2,3},聂国权^{2,3}

(1. 中国石油西南油气田分公司勘探开发研究院,四川成都 610041; 2. 中国地质科学院岩溶地质研究所/自然资源部、广西岩溶动力学重点实验室/联合国教科文组织国际岩溶研究中心,广西桂林 541004;
3. 广西平果喀斯特生态系统国家野外科学观测研究站,广西平果 531406)

摘要:近年来,高石梯—磨溪地区灯影组天然气勘探取得重要发现,其含气储层主要位于灯四段,储层岩石类型以藻凝块白云岩、藻砂屑白云岩、藻叠层白云岩为主。为了研究该地区灯影组白云岩的溶蚀差异,本文采用岩石切片和薄片同时进行溶蚀实验的方法,实验过程中定时记录实验数据,对灯影组白云岩的溶蚀速率、表面形貌和微观特征进行研究。实验结果既有溶蚀量化指标——溶蚀速率,又能直观掌握溶蚀特征及溶蚀后的孔隙结构变化。溶蚀实验结果表明:①所有样品的溶蚀启动速率均较高,随溶蚀时间增加,溶蚀速率呈现大幅度衰减并趋于稳定;②不同样品的溶蚀速率有明显差异,藻叠层白云岩、藻砂屑白云岩溶蚀速率最高,藻凝块白云岩次之,藻叠层硅质白云岩溶蚀速率最低;③通过观察比较不同反应时间内样品的微观溶蚀特征,发现沿粒间、晶间孔隙以及微裂隙溶蚀程度较高;④灯影组藻白云岩储层发育可能与藻间白云石的溶蚀作用有关。通过溶蚀实验,掌握了研究区不同白云岩的溶蚀差异,进而对预测优质储层分布、指导油气勘探具有重要意义。

关键词:四川盆地;灯影组;白云岩;溶蚀实验;溶蚀机理;碳酸盐岩储层

中图分类号:P618.13 **文献标识码:**A

文章编号:1001—4810(2023)06—1312—10

开放科学(资源服务)标识码(OSID):



0 引言

碳酸盐岩储层是一种重要的油气储层类型,据统计,全球碳酸盐岩油气藏储量约占油气资源总量的 50%,产量占 60% 以上^[1]。碳酸盐岩的溶蚀作用是指流动的可溶性流体与碳酸盐岩之间相互作用的过程及产生的结果,从地表到深埋藏地层中均可发生^[2-3]。碳酸盐岩溶蚀形成的溶孔、溶洞和溶缝是重要的油气储集空间,我国海相碳酸盐岩油气勘探实

践也证明了这一认识^[4-8]。

碳酸盐岩溶蚀实验是研究碳酸盐岩溶蚀有利条件和分布规律的重要方法^[9]。20世纪 70 年代以来,国内外学者陆续开展了碳酸盐岩溶蚀模拟实验,探讨成分、结构、温度、压力、流体等因素对溶蚀作用的影响^[10-17]。早期的溶蚀实验主要模拟地表环境进行实验,实验温度小于 100 ℃。20世纪 80 年代,国内外学者主要研究深埋藏环境下碳酸盐岩溶蚀机理,实验方法采用流体与岩石颗粒或块体之间的表面反

资助项目:中国地质调查局地质调查项目(DD20190723、DD20221658);中石油“高磨地区灯四段台内产能主控因素及开发目标优选技术研究”项目(20190303-06);广西重点研发计划项目(桂科 AB23026062)

第一作者简介:罗文军(1981—),博士,高级工程师,主要从事开发地质研究工作。E-mail: luowenjun@petrochina.com.cn。

通信作者:季少聪(1994—),硕士,助理研究员,主要从事古岩溶油气储层研究工作。E-mail: jishaocong00@163.com。

收稿日期:2023—01—23

应方式。近年来, 随着实验技术的进步, 已有学者陆续开展碳酸盐岩内部溶蚀实验^[12]。

前人对四川盆地高石梯—磨溪地区灯影组白云岩开展了较多的储层研究, 但主要集中在储层特征、古地貌刻画、气藏产能等方面, 缺乏白云岩溶蚀的模拟实验研究。本文以高石梯—磨溪地区灯影组藻白云岩为研究对象, 采用岩石切片和薄片同时进行溶蚀实验的方法, 通过对样品在溶蚀实验前后的溶蚀速率、表面形貌和微观特征, 分析岩性、结构、反应时间对白云岩溶蚀程度的影响。在此

基础上, 重点分析藻对白云岩溶蚀的作用机理, 为研究区藻白云岩溶蚀孔隙成因及发育特征研究提供实验依据。

1 地质概况

高石梯—磨溪地区位于四川省中部遂宁市、资阳市、重庆市潼南县境内(图 1)。构造上位于四川盆地中部, 处于川中古隆中斜平缓带的中部、乐山—龙女寺加里东古隆起东段的上斜坡部位^[18]。

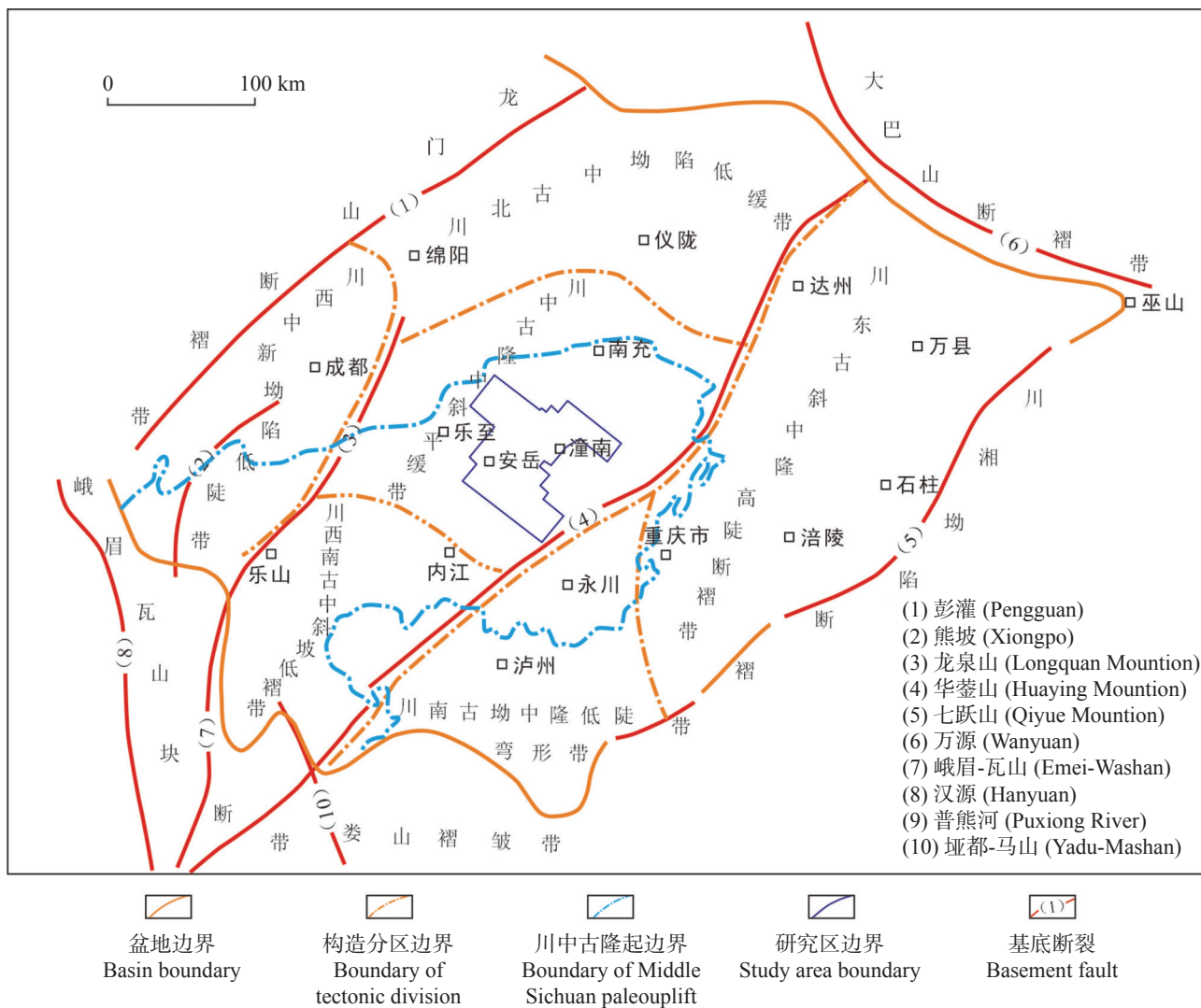


图 1 高石梯—磨溪地区构造位置图^[11]

Fig. 1 Tectonic location of the Gaoshiti-Moxi area

高石梯—磨溪地区灯影组发育厚层的藻白云岩、晶粒白云岩、砂屑和鲕粒白云岩夹薄层砂岩、泥岩和硅质岩, 主要为台地边缘礁滩相和局限台地潮坪—泻湖相沉积^[19]。根据岩性和岩石结构特征的不同, 灯影组从下至上可分为灯一段、灯二段、灯三段

和灯四段^[19]: 灯一段以泥粉晶白云岩、蓝藻细菌白云岩为主, 局部发育少量膏盐和纹层状构造; 灯二段以藻白云岩为主, 夹粉晶白云岩、泥晶白云岩和粒屑白云岩, 具斑马状、叠层状、雪花状、团块状及葡萄状结构, 局部夹膏盐岩及膏质、硅质白云岩; 灯三段以

泥页岩、泥质白云岩及硅质岩为主；灯四段主要由泥晶白云岩、粉晶白云岩、含砂屑白云岩、藻白云岩（包括藻叠层白云岩、藻凝块白云岩及藻砂屑白云岩等）组成，局部夹薄层灰黑色硅质条带。

整体上，灯四段岩溶储层发育，是目前灯影组勘探开发的主要目的层。灯四段藻凝块白云岩、泥粉晶白云岩在地层中发育程度最高，藻砂屑白云岩、藻叠层白云岩次之，而藻凝块白云岩储集性能最好，藻砂屑白云岩、藻叠层白云岩次之，泥粉晶白云岩储集性能最差。通过对高石梯—磨溪地区灯影组不同岩石类型的物性统计可以看出，藻含量最高的藻叠层白云岩平均孔隙度达4.88%，明显高于其他类型的白云岩，同时藻含量相对较高的藻砂屑白云岩、藻凝块白云岩、藻纹层白云岩的孔隙度整体高于泥晶白云岩、泥质白云岩和白云质泥岩（图2）。

2 样品采集与实验方法

为了研究高石梯—磨溪地区灯影组白云岩溶蚀差异，本次实验样品除采自高石梯—磨溪地区灯影

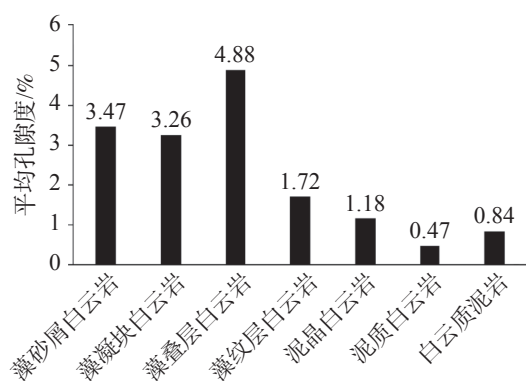


图2 灯四段不同岩类平均孔隙度直方图

Fig. 2 Histogram of average porosity of different rocks in the fourth member of Dengying Formation

组藻白云岩外，还采集了该区龙王庙组白云岩和广西环江上纳村石炭系白云岩样品作对比分析。白云岩薄片鉴定岩性分别为藻砂屑白云岩、藻叠层硅质白云岩、藻叠层白云岩、含藻白云岩、藻凝块白云岩、细中晶白云岩和细晶白云岩，溶蚀实验样品典型岩心照片如图3。

根据前人研究认为，研究区灯影组白云岩主要受暴露岩溶影响^[20]，所以本次室内溶蚀实验条件设

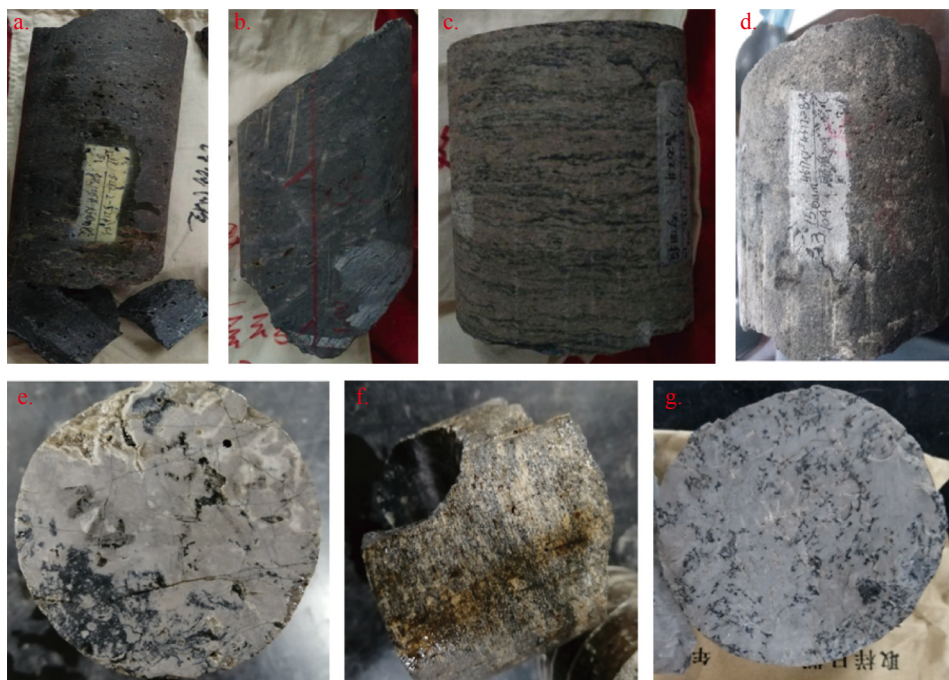


图3 实验样品典型岩心照片

a. GS1, 藻砂屑白云岩 b. GS2, 藻叠层硅质白云岩 c. GS3, 藻叠层白云岩 d. MX4, 细中晶白云岩 e. MX1, 含藻白云岩, 藻含量在10%左右
f. MX2, 藻凝块白云岩, 藻含量大于50% g. MX3, 藻凝块白云岩, 藻含量大于70%

Fig. 3 Typical core photos of experimental samples

a. GS1, algal arenaceous dolomite b. GS2, algal-laminated siliceous dolomite c. GS3, algal-laminated dolomite d. MX4, fine-to-medium-grained dolomite
e. MX1, algae-bearing dolomite with algae content of 10% f. MX2, algal agglomerate dolomite with algal content more than 50%
g. MX3, algal agglomerate dolomite with algal content more than 70%

定为常压条件, 为了加快实验进度, 采用 pH=4 的盐酸水溶液为反应溶液, 实验温度为 50 ℃, 在电热恒温振荡水槽中进行。实验主要比较不同岩性及结构对溶蚀作用的影响, 因此各组实验均采用相同的温度、压力和流体条件。具体实验内容和步骤如下:

(1) 首先将每个样品分别加工成圆柱体切片和岩石薄片两种类型;

(2) 用游标卡尺测量每个圆柱体切片不同位置的直径、厚度, 并求取平均值, 进而计算每个圆柱体切片的表面积, 溶蚀实验样品直径、厚度及表面积计算结果如表 1;

(3) 用超纯水清洗圆柱体切片, 在恒温干燥箱中烘干 2 h, 设定温度为 105 ℃。干燥完毕后, 将样品放在干燥皿中冷却, 再用分析天平称量每个圆柱体

切片的重量;

(4) 用相机分别对每个圆柱体切片进行拍照; 用偏光显微镜观察每个薄片的微观特征, 包括成分、结构、孔隙及裂隙发育情况等;

(5) 配置 pH=4 的盐酸水溶液, 将每个样品的圆柱体切片和薄片放置在相同烧杯中, 倒入配置好的盐酸水溶液, 再将烧杯放置在恒温振荡水槽中, 设置温度为 50 ℃, 进行溶蚀实验;

(6) 溶蚀实验分别进行 1 h、2 h、3 h、6 h、12 h、15 h、21 h、27 h、37 h、165 h 和 235 h 后, 取出样品, 重复步骤(3)、(4)、(5), 记录不同时间样品溶蚀后的重量、表面形貌及微观特征, 计算不同反应时间圆柱体切片单位面积的溶蚀速率, 溶蚀速率计算结果如表 2 所示。

表 1 实验样品直径、厚度及表面积计算结果

Table 1 Calculation results of diameters, thicknesses and surface areas of experimental samples

编号	岩性	地层	直径/cm	厚度/cm	表面积/cm ²
GS1	藻砂屑白云岩	灯影组	2.81	0.38	15.77
GS2	藻叠层硅质白云岩	灯影组	2.81	0.39	15.84
GS3	藻叠层白云岩	灯影组	2.82	0.42	16.17
MX1	含藻白云岩	灯影组	2.51	0.52	13.98
MX2	藻凝块白云岩	灯影组	2.42	0.47	12.81
MX3	藻凝块白云岩	灯影组	2.42	0.64	14.04
MX4	细中晶白云岩	龙王庙组	2.82	0.42	16.15
HD1	细晶白云岩	石炭系	2.80	0.40	15.89

表 2 实验样品地层、岩性及溶蚀速率计算结果

Table 2 Lithology, formation and calculation results of dissolution rates of experimental samples

编号	岩性	地层	溶蚀速率($10^{-4} \text{ g}\cdot\text{cm}^{-2}\cdot\text{d}^{-1}$)										
			1 h	2 h	3 h	6 h	12 h	15 h	21 h	27 h	37 h	165 h	235 h
GS1	藻砂屑白云岩	灯影组	126.17	17.05	19.02	5.63	2.82	7.81	2.26	3.15	1.16	0.42	0.02
GS2	藻叠层硅质白云岩	灯影组	47.13	7.27	8.18	3.03	1.54	/	4.07	2.07	0.82	0.29	0.16
GS3	藻叠层白云岩	灯影组	166.18	21.96	27.89	3.71	1.85	11.62	/	4.92	/	0.40	0.01
MX1	含藻白云岩	灯影组	165.64	31.33	38.19	0.86	3.29	/	/	0.66	/	/	/
MX2	藻凝块白云岩	灯影组	73.98	7.96	19.2	7.65	3.43	/	/	1.34	/	/	/
MX3	藻凝块白云岩	灯影组	66.23	34.18	21.36	2.85	0	/	/	0.54	/	/	/
MX4	细中晶白云岩	龙王庙组	175.8	50.38	/	8.22	2.30	10.25	0.79	5.10	0.21	0.41	0.63
HD1	细晶白云岩	石炭系	72.35	39.27	/	3.22	2.87	3.63	2.37	1.23	2.31	0.22	0.24

3 实验结果

3.1 溶蚀速率

根据溶蚀速率的计算结果(表 2, 图 4), 对比分

析不同样品、不同反应时间的溶蚀速率, 结果表明:

(1) 在实验条件下, 所有样品的溶蚀速率较小, 量级为 $10^{-4} \text{ g}\cdot\text{cm}^{-2}\cdot\text{d}^{-1}$, 溶蚀过程较缓慢;

(2) 所有样品在实验初期均有较高的溶蚀启动

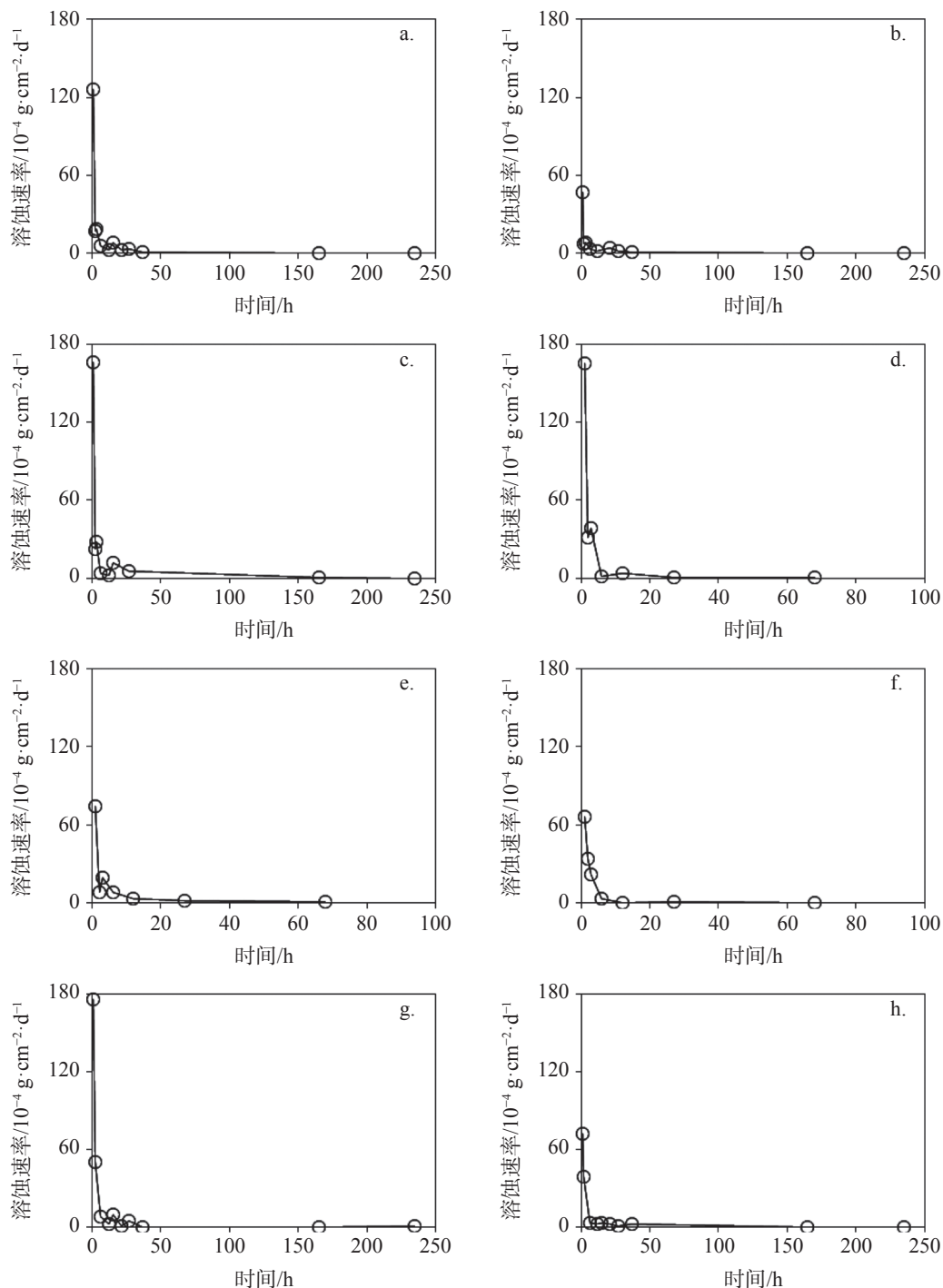


图 4 样品溶蚀速率随时间变化曲线

a. GS1, 藻砂屑白云岩 b. GS2, 藻叠层硅质白云岩 c. GS3, 藻叠层白云岩 d. MX1, 含藻白云岩, 藻含量在 10% 左右 e. MX2, 藻凝块白云岩, 藻含量大于 50% f. MX3, 藻凝块白云岩, 藻含量大于 70% g. MX4, 细中晶白云岩 h. HD1, 细晶白云岩

Fig. 4 Dissolution rate curve of samples with time variation

a. GS1, algal arenaceous dolomite b. GS2, algal-laminated siliceous dolomite c. GS3, algal-laminated dolomite d. MX1, algae-bearing dolomite with algae content of 10% e. MX2, algal agglomerate dolomite with algal content more than 50% f. MX3, algal agglomerate dolomite with algal content more than 70% g. MX4, fine-to-medium-grained dolomite h. HD1, fine grained dolomite

速率, 达 $45 \times 10^{-4} \sim 175 \times 10^{-4}$ g·cm $^{-2}$ ·d $^{-1}$; 随溶蚀时间增加, 所有样品的溶蚀速率均呈现大幅度衰减, 在 12 h 左右逐渐稳定于 $1.5 \times 10^{-4} \sim 3.5 \times 10^{-4}$ g·cm $^{-2}$ ·d $^{-1}$, 多数样

品在 27 h 后几乎不发生溶蚀;

(3) 不同样品的溶蚀启动速率有明显差异, 具体表现为 MX4(细中晶白云岩)、GS3(藻叠层白云岩)、

MX1(含藻白云岩)溶蚀速率最高, 介于 $165 \times 10^{-4} \sim 175 \times 10^{-4} \text{ g} \cdot \text{cm}^{-2} \cdot \text{d}^{-1}$ 之间; GS1(藻砂屑白云岩)溶蚀速率较高, 达 $126.17 \times 10^{-4} \text{ g} \cdot \text{cm}^{-2} \cdot \text{d}^{-1}$ 之间; MX2(藻凝块白云岩)、HD1(细晶白云岩)、MX3(藻凝块白云岩)溶蚀速率较低, 介于 $66 \times 10^{-4} \sim 74 \times 10^{-4} \text{ g} \cdot \text{cm}^{-2} \cdot \text{d}^{-1}$ 之间; GS2(藻叠层硅质白云岩)溶蚀速率最低, 达 $47.13 \times 10^{-4} \text{ g} \cdot \text{cm}^{-2} \cdot \text{d}^{-1}$ 之间。

3.2 微观变化特征

通过观察溶蚀实验前后圆柱体切片样品的表面形貌特征和薄片样品的微观特征, 对比分析不同样品、不同反应时间的溶蚀特征, 结果表明:

(1)所有样品在弱酸环境下均发生一定程度的溶蚀, 而不同岩性及结构的样品溶蚀程度有明显差异(图5)。GS1(藻砂屑白云岩)、MX4(细中晶白云岩)圆柱体切片样品在溶蚀后孔径明显增大, 孔隙之间可见短距离相互连通; GS3(藻叠层白云岩)圆柱体切片样品在溶蚀后样品表面变模糊;

(2)通过比较溶蚀实验前后圆柱体切片样品的溶蚀程度(图5), 可知 GS1(藻砂屑白云岩)、MX4(细中晶白云岩)溶蚀程度较高; GS3(藻叠层白云岩)次之, GS2(藻叠层硅质白云岩)溶蚀程度最低, 这与溶蚀速率的计算结果基本吻合。



图5 圆柱体切片样品溶蚀前后照片

a. 实验前, GS1, 藻砂屑白云岩 b. 实验后, GS1, 藻砂屑白云岩 c. 实验前, GS2, 藻叠层硅质白云岩 d. 实验后, GS2, 藻叠层硅质白云岩 e. 实验前, GS3, 藻叠层白云岩 f. 实验后, GS3, 藻叠层白云岩 g. 实验前, MX4, 细中晶白云岩 h. 实验后, MX4, 细中晶白云岩

Fig. 5 Photos of cylinder slice samples before and after dissolution

a. before the experiment, GS1, algal arenaceous dolomite b. after the experiment, GS1, algal arenaceous dolomite c. before the experiment, GS2, algal-laminated siliceous dolomite d. after the experiment, GS2, algal-laminated siliceous dolomite e. before the experiment, GS3, algal-laminated dolomite f. after the experiment, GS3, algal-laminated dolomite g. before the experiment, MX4, fine-to-medium-grained dolomite h. after the experiment, MX4, fine-to-medium-grained dolomite

4 讨论

4.1 孔隙、裂隙对白云岩溶蚀的影响

粒间孔隙、晶间孔隙发育的样品, 沿粒间、晶间孔隙溶蚀程度较高。溶蚀实验前, GS1(藻砂屑白云岩)样品圆柱体切片下孔隙主要呈孤立分布, 孔径较少且发育稀少(图5a); 溶蚀实验后, 孔径增大, 孔隙之间可见短距离相互连通, 连接通道以晶间裂隙为主, 但范围小, 且不稳定(图5b)。另外, 溶蚀实验后, MX4(细中晶白云岩)样品圆柱体切片表面也可见明

显的溶蚀扩大现象(图5g、h)。

微裂隙发育的样品, 沿微裂隙溶蚀程度较高。溶蚀实验前, 镜下观察可知 GS2(藻叠层硅质白云岩)样品局部发育微裂隙, 但微裂隙延伸短, 储集空间小(图6a); 溶蚀实验后, 微裂隙明显扩宽、延长, 储集空间明显增大(图6d)。

4.2 藻对白云岩溶蚀的影响

溶蚀实验后, GS2(藻叠层硅质白云岩)样品藻叠层间白云石晶粒发生明显溶蚀, 晶粒体积明显减少(图6b、e)。GS3(藻叠层白云岩)样品表面变模糊

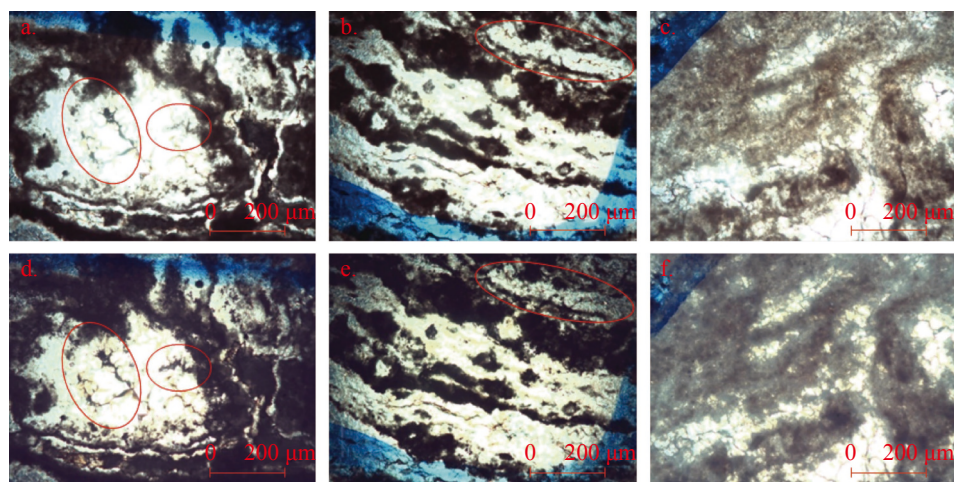


图 6 样品溶蚀前后微观特征

a. 实验前, GS2, 藻叠层硅质白云岩, 红圈为微裂隙 b. 实验前, GS2, 藻叠层硅质白云岩, 红圈为白云石晶粒 c. 实验前, GS3, 藻叠层白云岩 d. 实验后, GS2, 藻叠层硅质白云岩, 微裂隙发生扩溶 e. 实验后, GS2, 藻叠层硅质白云岩, 白云石晶粒发生溶蚀 f. 实验后, GS3, 藻叠层白云岩, 样品表面变模糊

Fig. 6 Microscopic characteristics of samples before and after dissolution

a. before the experiment, GS2, algal-laminated siliceous dolomite (red circle: microcrack) b. before the experiment, GS2, algal-laminated siliceous dolomite (red circle: dolomite grain) c. before the experiment, GS3, algal-laminated dolomite d. after the experiment, GS2, algal-laminated siliceous dolomite (The microcracks are dissolved.) e. after the experiment, GS2, algal-laminated siliceous dolomite (The dolomite grains are dissolved.) f. after the experiment, GS3, algal-laminated dolomite (The sample surface becomes blurred.)

(图 5e、f, 图 6c、f), 推测可流体难以进入样品内部进行较大规模溶蚀, 而仅在样品表面发生溶蚀。MX3 (藻凝块白云岩) 样品的溶蚀程度随着溶蚀时间的增加而增大, 白云石晶粒逐渐发生溶蚀。溶蚀实验前,

MX3(藻凝块白云岩) 样品的白云岩晶粒团块完整, 发育小型晶间孔(图 7a);在溶蚀时间达到 5 小时之后, 前期晶间孔明显增大, 底部位置可见溶蚀孔发育(图 7b);在溶蚀时间达到 12 小时之后, 底部溶蚀孔

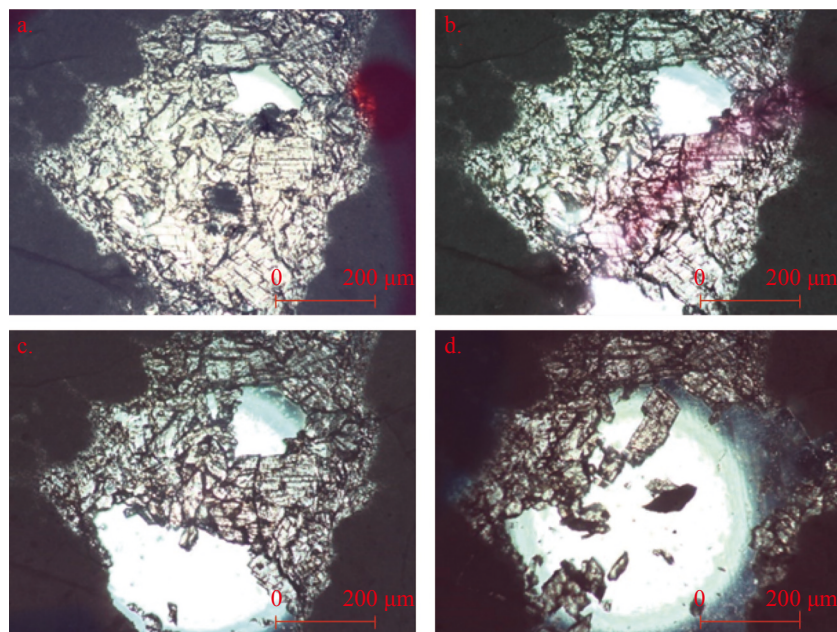


图 7 不同溶蚀时间藻凝块白云岩变化特征

a. 实验前, MX3, 藻凝块白云岩 b. 实验 5 h 后, MX3, 藻凝块白云岩 c. 实验 12 h 后, MX3, 藻凝块白云岩 d. 实验 18 h 后, MX3, 藻凝块白云岩

Fig. 7 Variation characteristics of algal agglomerate dolomite with different dissolution time

a. before the experiment, MX3, algal agglomerate dolomite b. after 5 hours of experiment, MX3, algal agglomerate dolomite c. after 12 hours of experiment, MX3, algal agglomerate dolomite d. after 18 hours of experiment, MX3, algal agglomerate dolomite

已明显扩大, 约占整个白云石晶粒团块的三分之一(图 7c); 在溶蚀时间达到 18 小时之后, 白云石晶粒团块发生破碎、变形, 溶蚀孔扩大、连通, 与溶蚀实验前相比有着显著差别(图 7d)。

通过镜下观察可以看出, 在成分上藻白云岩中主要发生溶蚀的成分是藻间的白云石, 可见白云石晶粒发生溶蚀, 晶粒体积减小, 微孔隙、微裂隙等发生扩溶; 而藻类的溶蚀程度整体较低, 未见明显的溶蚀孔隙、裂隙等现象(图 6、图 7)。综上分析认为, 高石梯—磨溪地区灯影组藻白云岩储层发育可能与藻间白云石的溶蚀作用有关, 藻间白云石溶蚀形成了大量的溶蚀孔隙, 最终形成了现今灯影组岩溶储层多发育于藻含量较高的藻白云岩的面貌。

5 结论及意义

(1) 所有样品均有较高的溶蚀启动速率, 随溶蚀时间增加, 呈现大幅度衰减并趋于稳定。不同样品的溶蚀速率有明显差异, 藻叠层白云岩、藻砂屑白云岩溶蚀速率最高, 藻凝块白云岩次之, 藻叠层硅质白云岩溶蚀速率最低。

(2) 通过观察比较不同反应时间样品微观溶蚀特征, 发现沿粒间、晶间孔隙以及微裂隙溶蚀程度较高, 灯影组藻白云岩储层发育可能与藻间白云石的溶蚀作用有关。

(3) 实验过程中定时记录实验数据, 可以准确认识溶蚀孔隙、裂隙形成及演变过程。采用岩石切片和薄片同时进行溶蚀实验的方法, 实验结果既有溶蚀量化指标—溶蚀速率, 又可掌握溶蚀结构变化, 可以更全面的理解溶蚀规律。

参考文献

- [1] Gledhill D K, Morse J W. Calcite dissolution kinetics in Na-Ca-Mg-Cl brines[J]. *Geochimica et Cosmochimica Acta*, 2006, 70(23): 5802-5813.
- [2] Sanders D. Syndepositional dissolution of calcium carbonate in neritic carbonate environments: Geological recognition, processes, potential significance[J]. *Journal of African Earth Sciences*, 2003, 36(3): 99-134.
- [3] 夏日元, 唐健生, 罗伟权, 邓自强, 关碧珠. 油气田古岩溶与深岩溶研究新进展[J]. 中国岩溶, 2001, 20(1): 76.
- [4] 马永生, 何登发, 蔡勋育, 刘波. 中国海相碳酸盐岩的分布及油气地质基础问题[J]. 岩石学报, 2017, 33(4): 1007-1020.
- MA Yongsheng, HE Dengfa, CAI Xunyu, LIU Bo. Distribution and fundamental science questions for petroleum geology of marine carbonate in China[J]. *Acta Petrologica Sinica*, 2017, 33(4): 1007-1020.
- [5] 何治亮, 张军涛, 丁茜, 尤东华, 彭守涛, 朱东亚, 钱一雄. 深层—超深层优质碳酸盐岩储层形成控制因素[J]. 石油与天然气地质, 2017, 38(4): 633-644, 763.
- HE Zhiliang, ZHANG Juntao, DING Qian, YOU Donghua, PENG Shoutao, ZHU Dongya, QIAN Yixiong. Factors controlling the formation of high-quality deep to ultra-deep carbonate reservoirs[J]. *Oil & Gas Geology*, 2017, 38(4): 633-644, 763.
- [6] 赵文智, 沈安江, 胡素云, 张宝民, 潘文庆, 周进高, 汪泽成. 中国碳酸盐岩储集层大型化发育的地质条件与分布特征[J]. 石油勘探与开发, 2012, 39(1): 1-12.
- ZHAO Wenzhi, SHEN Anjiang, HU Suyun, ZHANG Baomin, PAN Wenqing, ZHOU Jin'gao, WANG Zecheng. Geological conditions and distributional features of large-scale carbonate reservoirs onshore China[J]. *Petroleum Exploration and Development*, 2012, 39(1): 1-12.
- [7] 沈安江, 赵文智, 胡安平, 余敏, 陈娅娜, 王小芳. 海相碳酸盐岩储集层发育主控因素[J]. 石油勘探与开发, 2015, 42(5): 545-554.
- SHEN Anjiang, ZHAO Wenzhi, HU Anping, SHE Min, CHEN Yana, WANG Xiaofang. Major factors controlling the development of marine carbonate reservoirs[J]. *Petroleum Exploration and Development*, 2015, 42(5): 545-554.
- [8] 张庆玉, 梁彬, 秦凤蕊, 曹建文, 淡水, 李景瑞. 塔里木盆地奥陶系古潜山碳酸盐岩溶储层评价与预测: 以轮古7井区以东为例[J]. 中国岩溶, 2017, 36(1): 32-41.
- ZHANG Qingyu, LIANG Bin, QIN Fengrui, CAO Jianwen, DAN Yong, LI Jingrui. Evaluation and prediction of carbonate karst reservoirs in the Ordovician buried hills beneath the Tarim Basin: An example east of the Lungu7 well block[J]. *Carsologica Sinica*, 2017, 36(1): 32-41.
- [9] 余敏, 蒋义敏, 胡安平, 吕玉珍, 陈薇, 王永生, 王莹. 碳酸盐岩溶蚀模拟实验技术进展及应用[J]. 海相油气地质, 2020, 25(1): 12-21.
- SHE Min, JIANG Yimin, HU Anping, LYU Yuzhen, CHEN Wei, WANG Yongsheng, WANG Ying. The progress and application of dissolution simulation of carbonate rock[J]. *Marine Origin Petroleum Geology*, 2020, 25(1): 12-21.
- [10] 杨俊杰, 黄思静, 张文正, 黄月明, 刘桂霞, 肖林萍. 表生和埋藏成岩作用的温压条件下不同组成碳酸盐岩溶蚀成岩过程的实验模拟[J]. 沉积学报, 1995(4): 49-54.
- YANG Junjie, HUANG Sijing, ZHANG Wenzheng, HUANG Yueming, LIU Guixia, XIAO Linping. Experimental simulation of dissolution for carbonate with different composition under the conditions from epigenesis to burial diagenesis environment[J]. *Acta Sedimentologica Sinica*, 1995(4): 49-54.
- [11] 余敏, 朱吟, 沈安江, 郑兴平, 贺训云. 塔中北斜坡鹰山组碳酸盐岩溶蚀的模拟实验研究[J]. 中国岩溶, 2012, 31(3): 234-239.

- SHE Min, ZHU Yin, SHEN Anjiang, ZHENG Xingping, HE Xunyun. Simulation experiment for the dissolution of carbonate rocks of the Yingshan Formation on the northern slope of Tazhong uplift [J]. *Carsologica Sinica*, 2012, 31(3): 234-239.
- [12] 余敏, 寿建峰, 沈安江, 潘立银, 胡安平, 胡圆圆. 碳酸盐岩溶解规律与孔隙演化实验研究[J]. 石油勘探与开发, 2016, 43(4): 564-572.
- SHE Min, SHOU Jianfeng, SHEN Anjiang, PAN Liyin, HU Yuanyuan. Experimental simulation of dissolution law and porosity evolution of carbonate rock[J]. Petroleum Exploration and Development, 2016, 43(4): 564-572.
- [13] 蒋小琼. 普光与建南气田碳酸盐岩礁滩相储层埋藏溶蚀作用对比研究[D]. 武汉: 中国地质大学, 2014.
- JIANG Xiaoqiong. Contrastive research on the burial dissolution of carbonate reef-shoal reservoir rocks of Puguang and Jiannan gas fields in Sichuan basin[D]. Wuhan: China University of Geosciences, 2014.
- [14] 蒋小琼, 王恕一, 范明, 张建勇, 管宏林, 鲍云杰. 埋藏成岩环境碳酸盐岩溶蚀作用模拟实验研究[J]. *石油实验地质*, 2008, 30(6): 643-646.
- JIANG Xiaoqiong, WANG Shuyi, FAN Ming, ZHANG Jianyong, GUAN Honglin, BAO Yunjie. Study of simulation experiment for carbonate rocks dissolution in burial diagenetic environment[J]. *Petroleum Geology and Experiment*, 2008, 30(6): 643-646.
- [15] 彭军, 王雪龙, 韩浩东, 尹申, 夏青松, 李斌. 塔里木盆地寒武系碳酸盐岩溶蚀作用机理模拟实验[J]. *石油勘探与开发*, 2018, 45(3): 415-425.
- PENG Jun, WANG Xuelong, HAN Haodong, YIN Shen, XIA Qingsong, LI Bin. Simulation for the dissolution mechanism of Cambrian carbonate rocks in Tarim Basin, NW China[J]. *Petroleum Exploration and Development*, 2018, 45(3): 415-425.
- [16] 谭飞, 张云峰, 王振宇, 董兆雄, 黄正良, 王前平, 高君微. 鄂尔多斯盆地奥陶系不同组构碳酸盐岩埋藏溶蚀实验[J]. *沉积学报*, 2017, 35(2): 413-424.
- [17] TAN Fei, ZHANG Yunfeng, WANG Zhenyu, DONG Zhaoxiong, HUANG Zhengliang, WANG Qianping, GAO Junwei. Simulation experiment for the burial dissolution of different petrofabric carbonate rocks of Ordovician in the Ordos basin[J]. *Acta Sedimentologica Sinica*, 2017, 35(2): 413-424.
- 范明, 蒋小琼, 刘伟新, 张建勇, 陈红宇. 不同温度条件下CO₂水溶液对碳酸盐岩的溶蚀作用[J]. *沉积学报*, 2007(6): 825-830.
- FAN Ming, JIANG Xiaoqiong, LIU Weixin, ZHANG Jianyong, CHEN Hongyu. Dissolution of carbonate rocks in CO₂ solution under the different temperatures[J]. *Acta Sedimentologica Sinica*, 2007(6): 825-830.
- [18] 闫海军, 彭先, 夏钦禹, 徐伟, 罗文军, 李新豫, 张林, 朱秋影, 朱迅, 刘曦翔. 高石梯—磨溪地区灯影组四段岩溶古地貌分布特征及其对气藏开发的指导意义[J]. *石油学报*, 2020, 41(6): 658-670.
- YAN Haijun, PENG Xian, XIA Qinyu, XU Wei, LUO Wenjun, LI Xinyu, ZHANG Lin, ZHU Qiuying, ZHU Xun, LIU Xixiang. Distribution features of ancient karst landform in the fourth member of the Dengying Formation in the Gaoshiti-Moxi region and its guiding significance for gas reservoir development[J]. *Acta Petrolei Sinica*, 2020, 41(6): 658-670.
- [19] 邓月锐. 四川盆地高石梯构造灯影组储层特征研究[D]. 成都: 西南石油大学, 2013.
- DENG Yuerui. Reservoirs characterization for the Sinian Dengying Formation of Gaoshiti area in Sichuan basin[D]. Chengdu: Southwest Petroleum University, 2013.
- [20] 刘曦翔, 淡永, 罗文军, 梁彬, 徐亮, 聂国权, 季少聪. 四川盆地高石梯地区灯影组四段顶岩溶古地貌、古水系特征与刻画[J]. *中国岩溶*, 2020, 39(2): 206-214.
- LIU Xixiang, DAN Yong, LUO Wenjun, LIANG Bin, XU Liang, NIE Guoquan, JI Shaocong. Characterization of karst paleo-geomorphology and the paleo-water system on the top of the 4th member of the Dengying Formation in the Gaoshiti area, Sichuan basin[J]. *Carsologica Sinica*, 2020, 39(2): 206-214.

Experiment for the differential dissolution of dolomite of Sinian Dengying Formation in the Gaoshiti–Moxi area, the Sichuan basin

LUO Wenjun¹, JI Shaocong^{2,3}, LIU Xixiang¹, DAN Yong^{2,3}, LIANG Bin^{2,3}, NIE Guoquan^{2,3}

(1. Institute of Exploration and Development, PetroChina Southwest Oil and Gas Field Company, Chengdu, Sichuan 610041, China; 2. Institute of Karst Geology, CAGS/Key Laboratory of Karst Dynamics, MNR & GZAR/International Research Center on Karst under the Auspices of UNESCO, Guilin, Guangxi 541004, China; 3. Pingguo Guangxi, Karst Ecosystem, National Observation and Research Station, Pingguo, Guangxi 531406, China)

Abstract In recent years, important discoveries have been made in natural gas exploration of Dengying Formation in Gaoshiti–Moxi area of the Sichuan basin. The gas-bearing reservoirs are mainly located in the fourth member of the Dengying Formation, and the reservoir rock types are mainly algal agglomerate dolomite, algal arenaceous dolomite, and algal-laminated dolomite. Though many previous studies on the dolomite of Dengying Formation in the Gaoshiti–Moxi area of the Sichuan basin have been conducted, they mainly focus on reservoir characteristics,

paleogeomorphology characterization, gas reservoir productivity, etc. There are relatively few studies on simulation experiments of dolomite dissolution. The carbonate rock dissolution experiment is an important method to study the favorable conditions and distribution laws of carbonate rock dissolution. Since the 1970s, scholars at home and abroad have successively carried out simulation experiments of carbonate rock dissolution to explore the influence of composition, structure, temperature, pressure, fluid and other factors on dissolution. Early dissolution experiments mainly simulated surface environments, with experimental temperatures below 100 °C. In the 1980s, scholars at home and abroad mainly studied the dissolution mechanism of carbonate rock in a deep burial environment. The experimental method was the surface reaction between fluid and rock particles or blocks.

This study takes the algal dolomite of the Dengying Formation in the Gaoshiti–Moxi area as the research object. The dissolution rate, surface morphology, and microscopic characteristics of the dolomite of Dengying Formation are studied based on dissolution experiments with rock slices and thin sections. Meanwhile, the effects of lithology, structure, and reaction time on the dissolution degree of the dolomite are analyzed. The experimental results can not only display the quantitative indicator of dissolution—the dissolution rate, but also directly demonstrate dissolution characteristics and changes in pore structure after dissolution. The results of the dissolution experiment indicate as follows. (1) All samples indicate high initial dissolution rates in the early stage of the experiment, and as the dissolution time increases, the dissolution rate shows a significant attenuation and then tends to stabilize. (2) All samples undergo a certain degree of dissolution in a weak acid environment, and there are significant differences in the degree of dissolution among samples with different lithology and structure. There are significant differences in dissolution rates among different samples. Dissolution rates of algal-laminated dolomite and algal arenaceous dolomite are the highest, followed by that of algal agglomerate dolomite, and the dissolution rate of algal-layered siliceous dolomite is the lowest. (3) Observation and comparison of the microscopic dissolution characteristics of samples at different reaction times show that samples developed with intergranular and inter-crystalline pores exhibited a higher degree of dissolution along these pores. Samples developed with microcracks exhibit a higher degree of dissolution along these microcracks. (4) Regular recording of experimental data during the experiment can accurately illustrate the formation and evolution of dissolution pores and fractures. Conducting dissolution experiments with rock slices and thin sections can not only provide quantitative indicators of dissolution rates, but also show changes in dissolution structure, enabling a more comprehensive understanding of dissolution laws. (5) The development of algal dolomite reservoirs in the Dengying Formation may be related to the dissolution of algal dolomite, because a large number of dissolution pores developed by the dissolution of algal dolomite ultimately formed the appearance of the current karst reservoirs of Dengying Formation, which were mostly developed in algal dolomite with high algal content. Through dissolution experiments, the differences in dissolution of different dolomites in the study area have been analyzed, which is of great significance for predicting the distribution of high-quality reservoirs and guiding oil and gas exploration.

Key words the Sichuan basin, Dengying Formation, dolomite, dissolution experiment, dissolution mechanism, carbonate reservoir

(编辑 张玲)